

DEALING WITH SEDIMENT TRANSPORT OVER PARTLY NON-ERODIBLE BOTTOMS

François RULOT

Hydraulics in Environmental and Civil Engineering (HECE), University of Liège, Belgium,
francois.rulot@ulg.ac.be

Benjamin DEWALS, Pierre ARCHAMBEAU, Michel PIROTTON, Sébastien ERPICUM
HECE, University of Liège, Belgium

ABSTRACT: In depth-averaged flow and morphodynamic models using a finite volume discretization based on explicit time integration, a specific difficulty can arise during a computation: the computed sediment level can become lower than the level of a non-erodible bottom. The original developments presented in this paper enable correction of the non-physical sediment levels. The method, based on iterative limitation of the outward fluxes, is perfectly mass conservative and remains computationally efficient. The resulting model has been validated with several 1D benchmarks leading to configurations with sediment transport over a non-erodible bottom. Two interesting experimental benchmarks are highlighted in this paper to show the efficiency of numerical simulations. In these benchmarks, the computation time has been verified not to increase by more than 15% when using the new method.

Keywords: non-erodible bottoms, numerical simulation, outward fluxes corrections.

INTRODUCTION

For decades, sediment transport has become a major topic of research because man-made structures (dams, weirs, channelization...) affect sediment transport continuity. Thus, sediment transport can have critical consequences for public safety, management of water resources, and sustainability of river systems. In order to deal correctly with these issues, morphological models should be able to simulate the wide range of flow features and sediment characteristics encountered in real-life applications. In this paper, we focus on one of them: modelling sediment transport and morphodynamics in domains including both erodible (alluvial) and non-erodible (non-alluvial) areas. Non-erodible bottoms refer to all areas that may not be set in motion under given hydraulic conditions (i.e. bed rocks, concrete structure, armoured layers, concrete slab...). In the present paper, an original mass-conservative iterative method, both simple and efficient, is introduced for 1D computation. This method, called the Flux Minimization Method (FMM), is inspired by the correction method for the negative water depth in flow computation (DEWALS et al. 2011). Compared to existing methods, FMM provides a good take-off between

computational time and accuracy in mass conservation (RULOT et al. 2011).

The mathematical and numerical model is first described (section 2), detailing the governing equations to which the FMM has been applied. The method is next explicitly described (section 3). In section 4, the numerical model is validated on two experimental benchmarks enabling to a better comprehension of the flow and sediment transport processes.

MATHEMATICAL AND NUMERICAL MODEL

In this section, the derivation of a 1D mathematical model for flow and morphodynamics is first explained. Then, the finite volume numerical technique applied to solve the set of governing equations is detailed.

Depth-averaged hydrodynamic and morphodynamic equations

Following an Eulerian description, depth-averaged 1D equations for flow and bed-load transport can be written in the following vector form:

$$\frac{\partial \mathbf{s}}{\partial t} + \frac{\partial \mathbf{f}_a}{\partial x} = \mathbf{r} \quad (1)$$

with:

$$\mathbf{s} = \left[h \quad h\bar{u} \quad (1-p)z_b \right]^T \quad (2)$$

$$\mathbf{f}_a = \left[h\bar{u} \quad h\bar{u}^2 + \frac{gh^2}{2} \quad q_{bx} \right]^T \quad (3)$$

$$\mathbf{r} = \left[0 \quad -g h \left(\frac{\partial z_b}{\partial x} + J \Delta \Sigma \right) \quad 0 \right]^T \quad (4)$$

Over bars denote depth-averaged quantities. t = time; u = velocity component along the flow direction x ; h = water depth; p = sediment porosity; z_b = bed level; g = gravity acceleration; q_{bx} = bed-load unit discharges along x ; J = the friction slope and:

$$\Delta \Sigma = \sqrt{1 + \left(\frac{\partial z_b}{\partial x} \right)^2} \quad (5)$$

Space and time discretization

The computation domain is discretized by means of a Cartesian grid, having thus the benefits of regular grids in terms of order of accuracy, computation time, and memory requirement.

The space discretization of the divergence form of Eqs. (1)–(4) is performed by means of a finite

volume scheme. Advective fluxes are computed by a Flux Vector Splitting (FVS) method (ERPICUM et al. 2010, DEWALS et al. 2008), which can be formally expressed as follows:

$$\mathbf{f}_a^+ = \left[h\bar{u} \quad h\bar{u}^2 \quad q_{bx} \right]^T ; \mathbf{f}_a^- = \left[0 \quad \frac{gh^2}{2} \quad 0 \right]^T \quad (6)$$

where the exponents + and – refer to, respectively, an upstream and a downstream evaluation of the corresponding terms on the finite volume edges. The time integration is performed here by means of a Runge-Kutta algorithm. For stability reasons, the time step is constrained by the Courant–Friedrichs–Levy (CFL) condition.

ORIGINAL METHOD TO HANDLE NON-ERODIBLE BOTTOMS

Exner equation [3rd component in Eq.(1)] provides the evolution of the sediment level as a function of bed-load fluxes, evaluated by means of a transport capacity formula. However, when solving conventionally the Exner equation in the presence of a partly non-erodible bed with explicit time integration, it may happen that the computed values of the bed elevation are found to be below the top of the non-erodible layer. Therefore, additional constraints must be prescribed on the sediment fluxes; to verify everywhere $z_b > z_b^F$ where z_b and z_b^F are the actual and non-erodible bed levels, respectively, while ensuring mass conservation.

Our original approach consists of an iterative procedure in which corrections affect only the cells in which the computed sediment level is below the rigid bottom. To ensure correct mass conservation in the resolution of Exner equation, a three-step procedure was used at each time step:

1. Exner Equation is evaluated (step 1 in Fig. 1).
2. The algorithm checks, among all cells, those in which the current sediment level, as obtained in step 1, is below the fixed bottom level. In those cells, the outflow discharge q_{bi}^{out*} is reduced (step 2 in Fig. 1; dashed arrow) such that the computed bed level becomes strictly equal to the rigid bottom level ($q_{bi}^{out} = q_{bi}^{out*} \alpha$). Regarding Fig. 1, step 1, the parameter α affecting the outward sediment flux in cell I is given by the following formula:

$$\alpha = \frac{\Delta x (1-p) (z_{bI}^0 - z_{bI}^F)}{\Delta t q_{bi+1}} + \frac{q_{bi}}{q_{bi+1}} \quad (7)$$

where Δx is the space step and Δt the time step. “I” refers to the index of the cell, while

“ i ” refers to the index of the edges.

- Since these flux corrections may in turn induce other non-physical configuration in neighboring cells, steps 1 and 2 are repeated iteratively. This leads eventually to a configuration in which the levels are all in their physical range, as shown in the final step in Fig. 1. Details on this method are available (RULOT et al. 2011).

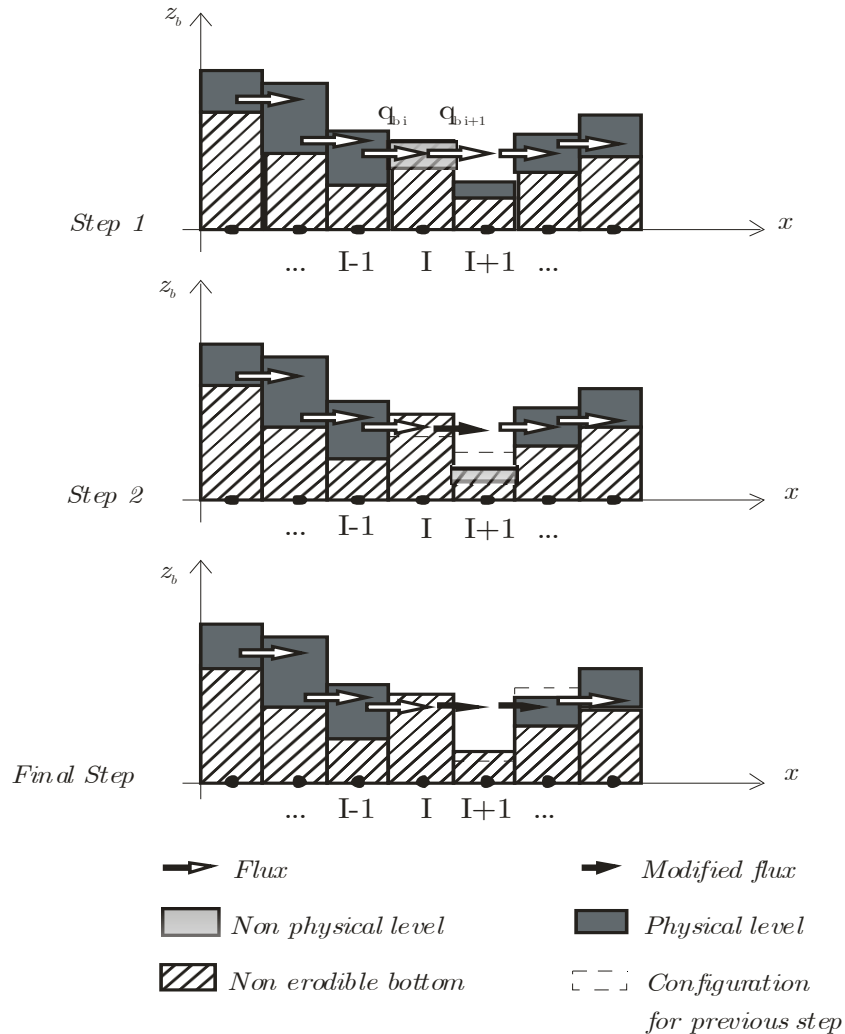


Figure 1 – Three steps procedure

VALIDATION

The cross section-averaged flow model combined with the algorithms of sediment flux correction have been verified and evaluated using several benchmarks leading to configurations with sediment transport over non-erodible bottoms. Comparison with two one-dimensional benchmarks is discussed below: first, the migration of trenches passing over a fixed bump, and then the evolution of the transport of a heap of sediments under simple flow conditions.

Evolution of a trench over a fixed bump

Description

This benchmark considers the evolution of a trench passing over a non-erodible bump (STRUIKSMA 1999). Two experiments were carried out. The length of the straight channel was 11.5 m and its width was 0.2 m. The discharge was 9.2 l/s and the water depth was 0.106 m. A bump was located in the middle of the domain, while an approximately 0.05-m-deep and 2-m-long trench was excavated in the alluvial bed upstream. The grain diameter was equal to 0.45 mm. STRUIKSMA (1999) assumed that the bed-load transport capacity formula is a power function of the water velocity: $q_{bx} = m u^5$ where $m = 3.6 \cdot 10^{-4} \text{ s}^4/\text{m}^3$ (test n°1) and $m = 4.0 \cdot 10^{-4} \text{ s}^4/\text{m}^3$ (test n°2) is a calibration parameter. The upstream sediment transport, including pores, is $q_{b,upstream} = 4.0 \text{ l/h}$ (test n°1) and $q_{b,upstream} = 4.4 \text{ l/h}$ (test n°2). The bottom Chézy friction coefficient $C_f = 31.8 \text{ m}^{1/2}/\text{s}$ was used to compute the friction slope. Numerically, the cell size is 0.1 m.

Results

Comparisons between numerical and experimental results are shown in Fig. 2. For both test cases, experimental data are scattered but the overall agreement with numerical predictions is found satisfactory. Looking deeper into the details (Fig. 2), computations over predict erosion depth downstream of the non-erodible bump for both tests. This may result from the simplified transport capacity formula used, accounting neither for an explicit threshold for transport inception nor for gravity-induced sediment transport. Vertical accelerations might also play a part in this region. Results of test n°1 and test n°2 also reveal that the computed sediment level on the bump is under predicted. The deeper sediment layer found experimentally may result from the medium-sized gravels used to build the bump (non-erodible under considered hydraulic conditions) leading to a higher bed roughness, which is not accounted for in the numerical model. The volume conservation error was, for both tests, lower than 10^{-10} m^3 , which is negligible. CPU time is at most 14% greater using FMM.

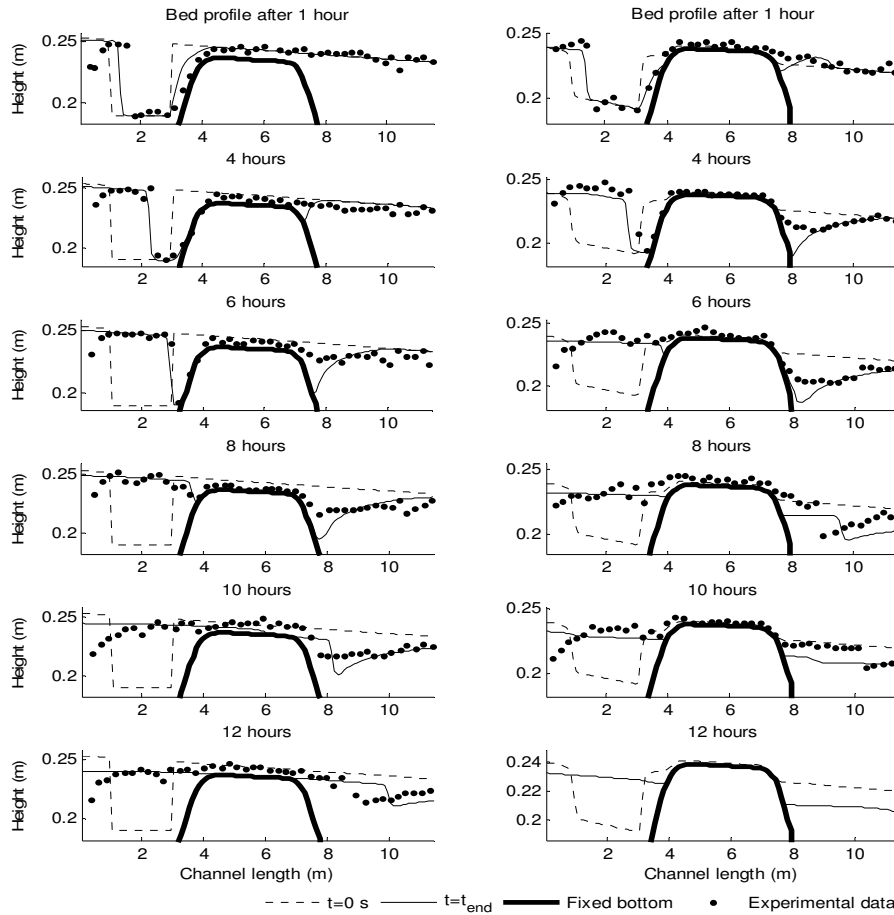


Figure 2 – Time evolution of the longitudinal bed profiles (Test n°1, left and test n°2, right)

Evolution of a heap of sediments

Description

The experimental study discussed in this section was carried out at the engineering hydraulics laboratory of the University of Liège using a rectangular horizontal channel 5.91 m long, 0.75 m high, and 0.15 m wide (CORNIL MOLINO 2011). Two reservoirs were located at the beginning and at the end of the channel to dissipate the energy, avoid boundary effects in the flow and collect sediments downstream. The sediments were plastic particles with a mean diameter of $d_{50} = 2.8$ mm and a density of 1045 kg/m^3 . The porosity between sediment was calculated to be 0.34. The Strickler friction coefficient (K) was calculated to (JAEGER 1956):

$$K = \frac{21}{d_{90}^{1/6}} = \frac{21}{0.0034^{1/6}} \simeq 54 \text{ m}^{1/3} \cdot \text{s}^{-1} \quad (8)$$

The diameter, d_i , accounts for the particle size, of which $i\%$ is smaller.

The sensitivity of two parameters was tested: the discharge varying between 5.85 and 7.85 l/s and the weight of sediment heap varying between 1 and 5 kg. The free surface level was set to 0.238 m. The discharge, Q_{eq} , was equal to 1.8 l/s at time $t = 0$ second and increased linearly during 60 seconds to reach a constant value of Q_{eq} . A 4-cm cell size was used. The Meyer-Peter Müller bed-load transport formula, in which the dimensionless critical shear stress for inception of motion is $\tau_{cr}^* = 0.03$, was solved. A Manning-Strickler formula was used to evaluate the friction slope. The main difference with the previous benchmark is that all parameters are physically-based or empirical.

Results

Comparisons between numerical and experimental results are shown in Fig. 3. Point 'A' is the beginning of the upstream slope of the dune, point 'B' is the end of the downstream slope of the dune, and the highest point of the dune is named the crest. The agreement between experimental data and numerical predictions was found satisfactory. The overall shape of the sediment heap is well reproduced. However, for the upstream face, the observed slope was milder and smoother than the numerical one. This observation is probably due to the vertical component of the velocity [15 % of the horizontal one (CORNIL MOLINO 2011)], which is not reproduced in the numerical model. For the downstream face, the slope was shaped by the gravity induced sediment motion rather than the flow induced sediment motion. Indeed, downstream of the dune crest, there is a recirculation zone leading to negative velocity along x direction. This was computed by activating only gravity induced sediment motion downstream of the sediment heap. The sensitivity tests show that the velocity of the sediment heap is directly linked to the water discharge. The sediment crest height is directly linked to the initial sediment heap height.

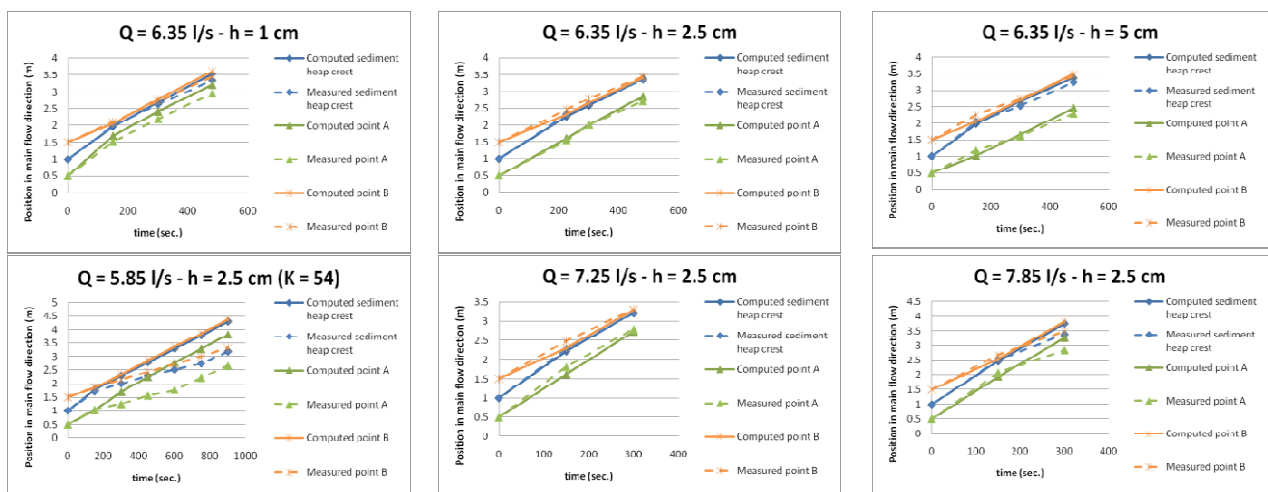


Figure 3 – Time evolution of the location of three points (A, B, crest)

Using the FMM, the sediment volume is conserved at the floating-point accuracy, while there is more than 184% error between initial and final volume when correcting the non-physical levels by simply putting it back at the non-erodible level. CPU time is 8% greater when using FMM.

CONCLUSIONS

Relying on a validated 1D numerical model to describe the flow and bed-load transport, an original algorithm has been developed in order to handle sediment transport on partly non-erodible bottoms. The method consists of limiting the outward fluxes in order to ensure that the sediment level remains higher than the non-erodible level on each cell of the domain. It has proved its efficiency in terms of computational time, as well as for respecting a non-erodible bottom constraint, while enabling verification of the sediment mass conservation close to the floating-point accuracy. Two benchmarks presented in this paper highlight the good agreement between numerical solutions and experimental observations. In addition, the increase in computational time is very limited for each benchmark. In the worst case, the computation time has been verified not to increase by more than 15% compared to the same simulation without a non-erodible bottom.

For further research, an interesting topic will be the corrections of computed sediment concentrations in suspended sediment transport in which the concentration of sediment in water must remain between zero and one.

REFERENCES

- CORNIL MOLINO, A. (2011), "Gestion des sédiments : opérations de chasses en géométrie idéalisée", Master Thesis, University of Liège, June 2011, 109 pages.
- DEWALS, B., RULOT, F., ERPICUM, S., ARCHAMBEAU, P. and PIROTON, M. (2011). "Advanced topics in sediment transport modelling: non-alluvial beds and hyperconcentrated flows", INTECH, 30 pages.
- DEWALS, B. J., KANTOUSH, S. A., ERPICUM, S., PIROTON, M. and SCHLEISS, A. J. (2008). "Experimental and numerical analysis of flow instabilities in rectangular shallow basins", *Environmental Fluid Mechanics*, Vol. 8, No. 1, pp 31-54.
- ERPICUM, S., DEWALS, B. J., ARCHAMBEAU, P. and PIROTON, M. (2010). "Dam-break flow computation based on an efficient flux-vector splitting", *Journal of Computational and Applied Mathematics*, Vol. 234, No. 7, pp 2143-2151.
- JAEGER, C. (1956). "Engineering fluid mechanics", Blackie, 548 pages.
- RULOT, F., DEWALS, B. J., ERPICUM, S., ARCHAMBEAU, P. and PIROTON, M. (2011).

"Modelling sediment transport over partially non erodible bottoms", International Journal for Numerical Methods in Fluids, Published Online: 10.1002/flid.2684.

STRUIKSMA, N. (1999). "Mathematical modelling of bedload transport over non-erodible layers", Proc. IAHR Symposium on River, Coastal and Estuarine Morphodynamics, Genova, Italy, pp 6-10.